Prepr. (*Am. Chem. Soc., Div. Polym. Chem.*) **1980**, *21*, 132. (c) Onder, B. K. US Patent 4,072,665, 1978.
(15) (a) Skrovanek, D. J.; Howe, S. E.; Painter, P. C.; Coleman, M. M. *Macromolecules* **1985**, *18*, 1676. (b) Skrovanek, D. J.; Painter, P. C.; Coleman, M. M. *Macromolecules* **1986**, *19*, 699.
(16) McGhie, A. R.; Kalyanaraman, P. S.; Garito, A. F. *Mol. Cryst. Liq. Cryst.* **1979**, *50*, 287.
(17) Ballistreri, A.; Garozzo, D.; Giuffrida, M.; Montaudo, G. *Macromolecules* **1987**, *20*, 2991.
(18) Babbit, G. E.; Patel, G. N. *Macromolecules* **1981**, *14*, 554.
(19) Havens, J. R.; Thakur, M.; Lando, J. B.; Koenig, J. L. *Macromolecules* **1984**, *17*, 1071.
(20) Wenz, G.; Muller, M. A.; Schmidt, M.; Wegner, G. *Macromolecules* **1984**, *17*, 837.
(21) Weeding, T. L.; Veeman, W. S.; Gaur, H. A.; Huysmans, W. G. B. *Macromolecules* **1988**, *21*, 2028.
(22) Tanaka, H.; Thakur, M.; Gomez, M. A.; Tonelli, A. E. *Macromolecules* **1987**, *20*, 3094.
(23) Lyerla, J. R. In *Polymers, Part A: Molecular Structure and Dynamics*; Fava, R. A., Ed.; Methods of Experimental Physics; Academic: New York, 1980; Vol. 16, Chapter 4.
(24) Komoroski, R. A. In *High Resolution NMR Spectroscopy of Synthetic Polymers in Bulk*; Komoroski, R. A., Ed.; VCH: Deerfield Beach, FL, 1986; Chapter 2.
(25) Torchia, D. A. *J. Magn. Reson.* **1978**, *30*, 613.
(26) See for example: (a) Bloor, D.; Hubble, C. L. *Chem. Phys. Lett.* **1978**, *56*, 89. (b) *Photon, Electron, and Ion Probes of Polymer Structure and Properties*; Dwight, D. W., Fabish, T. J., Thomas, H. R., Eds.; ACS Symposium Series 162; American Chemical Society: Washington, DC, 1981; pp 81–104.
(27) Rubner, M. F.; Sandman, D. J.; Velazquez, C. *Macromolecules* **1987**, *20*, 1296.
(28) (a) Patel, G. N.; Chance, R. R.; Witt, J. D. *J. Chem. Phys.* **1979**, *70*, 4387. (b) Patel, G. N.; Chance, R. R.; Witt, J. D. *J. Polym. Sci., Polym. Lett. Ed.* **1978**, *16*, 607. (c) Walters, G.; Painter, P.; Ika, P.; Frisch, H. *Macromolecules* **1986**, *19*, 888. (d) Chance, R. R.; Patel, G. N.; Witt, J. D. *J. Chem. Phys.* **1979**, *71*, 206.

Deuterium NMR Analysis of Poly(γ-benzyl L-glutamate) in the Lyotropic Liquid-Crystalline State: Orientational Order of the α-Helical Backbone and Conformation of the Pendant Side Chain

Akihiro Abe* and Toshimasa Yamazaki

Department of Polymer Chemistry, Tokyo Institute of Technology, 2-12-1 Ookayama, Meguro-ku, Tokyo 152, Japan.
Received June 9, 1988; Revised Manuscript Received October 14, 1988

ABSTRACT: Deuterium NMR studies have been performed on variously labeled PBLG samples in the lyotropic liquid-crystalline state: PBLG-*N-d*, -*α-d*, -*N,α-d*$_2$, -*α,β-d*$_3$, -*γ-d*$_2$, and -*benzyl-d*$_7$. The orientational order S of the α-helical backbone was estimated from the observed quadrupolar splittings $\Delta\nu$ of the N–D and C$^\alpha$–D bonds. The relative orientation of the side chains with respect to the backbone was elucidated by the rotational isomeric-state analysis of the $\Delta\nu/S$ data observed for the β-, γ-, and ζ-methylene and the *p*-benzyl deuterons. The most preferred conformation of the side chain was found to be $\chi_1\chi_2\chi_3\chi_4\chi_5$ = ttttt (31%) in 1,4-dioxane, ttttt (18%) in chloroform, and g$^-$tttt (20%) in *m*-cresol at 30 °C. The analysis also indicates that the steric overlaps between adjacent side chains play an important role in determining the preference of conformations in the PBLG system. The lateral dimension of the α-helical PBLG rod, expressed by the radius of gyration, was estimated to be 6.5 ± 0.1 Å, being substantially larger than those (3.5–4.8 Å) reported by Luzzati et al. using the SAXS method.

Introduction

In our preliminary communication,[1a] we have demonstrated that the deuterium NMR technique is useful in studying the molecular ordering of poly(γ-benzyl L-glutamate) (PBLG) in the lyotropic liquid-crystalline state. The orientational order parameter of the α-helical backbone has been elucidated as a function of concentration by using the PBLG samples deuterated at the amide group. In this treatment, the observed deuterium quadrupolar splitting $\Delta\nu$ has been related to the order of the uniaxial liquid crystal by the expression

$$S = (2/3)\Delta\nu/q_h \tag{1}$$

where S designates the degree of orientation defined as the second-order Legendre polynominal and q_h is the component of the quadrupolar interaction tensor along the α-helical axis

$$q_h = \left(\frac{e^2qQ}{h}\right)_{\rm ND}\left(\frac{3\cos^2\theta_{\rm N} - 1}{2} + \frac{\eta}{2}\sin^2\theta_{\rm N}\cos 2\phi_{\rm N}\right) \tag{2}$$

where $(e^2qQ/h)_{\rm ND}$ is the quadrupolar coupling constant of the N–D bond, η is the asymmetry parameter, and $\theta_{\rm N}$ and $\phi_{\rm N}$ are the angles which define the orientation of the α-helical axis in the Cartesian coordinate system affixed to the amide group (Figure 1): the z axis is taken to be parallel to the N–D bond, the x axis defined in the amide plane, and the y axis perpendicular to the plane.

The orientational order parameter of the α-helical backbone can also be deduced by introducing deuterium in the α-methine group. For the C$^\alpha$–D bond, the asymmetry parameter is known to be negligibly small, and thus

$$q_h = \left(\frac{e^2qQ}{h}\right)_{\rm CD}\left(\frac{3\cos^2\theta_\alpha - 1}{2}\right) \tag{3}$$

where $(e^2qQ/h)_{\rm CD}$ is the quadrupolar coupling constant of the C–D bond and θ_α designates the angle between the C$^\alpha$–D bond and the α-helical axis. In this paper, determination of the orientational order parameter of the α-helical axis has been attempted by using samples deuterated at the amide as well as α-methine group.[1b]

Under the experimental condition employed, PBLG molecules assume a nematic ordering. Samulski et al.[2,3] and Sohma et al.[4] have measured D NMR spectra of PBLG having partially or fully deuterated benzyl groups in the lyotropic liquid-crystalline state. From the observed quadrupolar splittings, they concluded that the orientation

0024-9297/89/2222-2138$01.50/0

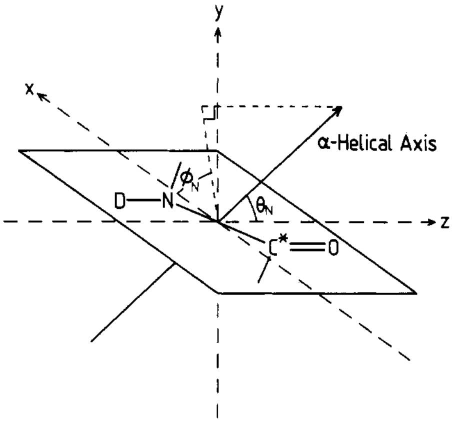

Figure 1. Cartesian coordinate system affixed to the amide group of PBLG-*N*-*d* and definition of spherical polar angles θ_N and ϕ_N.

of the side chain is also anisotropic. For a C–D bond of the side chain, the splitting $\Delta\nu$ can be expressed as

$$\Delta\nu = (3/2)\langle q_h \rangle S \tag{4}$$

$$\langle q_h \rangle = \left(\frac{e^2qQ}{h}\right)_{\mathrm{CD}} \left(\frac{3\langle \cos^2\theta\rangle - 1}{2}\right) \tag{5}$$

where ⟨ ⟩ designates an average taken over all conformations of the side chain and S represents the order parameter of the α-helical axis as defined in eq 1. As before, $(e^2qQ/h)_{\mathrm{CD}}$ is the quadrupolar coupling constant of a given C–D bond, and θ indicates the inclination of the C–D bond relative to the molecular axis. With the value of S obtained above, eq 4 yields the orientational order of a given C–D bond of the side chain. For the purpose of elucidating the average conformation of the side chain, we have prepared variously deuterated PBLG samples: PBLG-α,β-d_3, PBLG-γ-d_2, and PBLG-*benzyl*-d_7. Fractions of the conformer permitted under the experimental condition can be determined by adjusting the conformational statistical weight parameter of each rotatable bond so as to reproduce experimental values of $\Delta\nu$, the same technique being successfully employed in the D NMR analysis of thermotropic liquid crystals.[5] Comparison of the results with those calculated for a side chain isolated from its neighbors should provide information regarding the intramolecular side chain–side chain interactions.[1b]

Experimental Section

Preparation of Samples. PBLG. *N*-Carboxy-γ-benzyl L-glutamate anhydride (NCA) was prepared by a standard method and polymerized in 1,4-dioxane with triethylamine as initiator. The polypeptide formed was purified by repeated precipitation from a chloroform in a large volume of methanol. The molecular weights of PBLG samples were estimated from the intrinsic viscosities measured in dichloroacetic acid by using Doty et al.'s relation:[6] $[\eta] = 2.78 \times 10^{-5} M_v^{0.87}$.

PBLG-*N*-*d*. PBLG was dissolved in trifluoroacetic acid-*d* (TFA-*d*) and kept at room temperature for 1 h. The sample was precipitated into methanol and purified as above. The molecular weight of samples was found to remain practically unaffected by this treatment: $M_v = 27.5 \times 10^4$ and 7.3×10^4.

PBLG-α-*d*. L-Glutamic acid-α-*d* (deuterium content >97%, optical purity 100%) was prepared according to the method described by Hilton et al.[7] The polymer was obtained by the NCA method as stated above: $M_v = 6.8 \times 10^4$ and 5.7×10^4. Some of the PBLG-α-*d* samples were converted to PBLG-*N*,α-d_2 by treating with TFA-*d*.

PBLG-α-d_3. L-Glutamic acid-α,β-d_3 (deuterium content >97%, optical purity 100%) was synthesized according to Whelan et al.'s prescription.[8] PBLG-α,β-d_3 was prepared by the NCA method: $M_v = 11.3 \times 10^4$.

PBLG-γ-d_2. L-Glutamic acid-γ-d_2 (deuterium content 96%, optical purity 100%) was obtained as described by Tsutsumi et al.[9] PBLG-γ-d_2 was prepared by the NCA method: $M_v = 6.5 \times 10^4$.

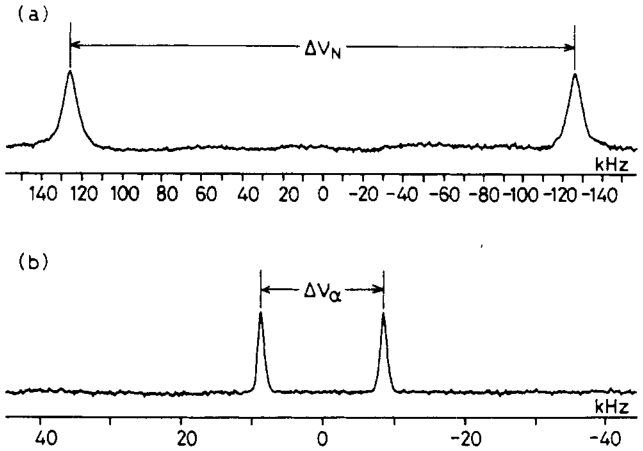

Figure 2. Typical examples of D NMR spectra observed in chloroform at 30 °C: (a) PBLG-*N*-*d* and (b) PBLG-α-*d*.

PBLG-*benzyl*-d_7. Preparation of PBLG samples carrying perdeuterated benzyl ester groups has been reported in a previous paper:[10] $M_v = 14.6 \times 10^4$.

Measurements. The D NMR spectra of liquid-crystalline solutions were recorded at 76.65 and 41.25 MHz, respectively, on JEOL JNM-GX-500 and JNM-GX-270 spectrometers equipped with variable-temperature controllers. Prior to the measurements, liquid-crystalline solutions were equilibrated in the spectrometer until homogeneous alignment was achieved. Measurements were carried out under a complete proton decoupling and nonspinning mode. The volume fraction of the sample, v_x, was estimated from the density (1.27 g cm^{-3}) of PBLG.

The D NMR powder pattern spectrum (46.06 MHz) was obtained for a solid sample of PBLG-*N*-*d* by using a Brucker CXP-300 spectrometer at room temperature, the quadrupolar-echo pulse sequence being $90°_x$–t–$90°_y$–t–echo.

Results and Discussion

Quadrupolar Coupling Constant. In our previous work,[1a] we used a set of parameters $(e^2qQ/h)_{\mathrm{ND}} = 210.8$ kHz and $\eta = 0.139$, the same values adopted in Chapman et al.'s paper.[11] These values were originally derived from Chiba's work[12] on the single crystal of urea-d_4. An attempt was also made to elucidate these parameters directly from the PBLG-*N*-*d* sample.[1b] The D NMR powder pattern has been obtained from the PBLG-*N*-*d* solid sample, which is free of any preferred orientations. Recently, Poliks et al.[13] reported a solid-state D NMR spectrum having a sharp profile, from which they estimated values of $(e^2qQ/h)_{\mathrm{ND}} = 201.9$ kHz and $\eta = 0.194$. Their values surpass our data[1b] in accuracy.

For the aliphatic and aromatic C–D bonds, values in the range $(e^2qQ/h)_{\mathrm{CD}} = 170 \pm 5$ and 185 ± 5 kHz, respectively, are used in the literature.[14] Values of 168.0 and 188.0 kHz, respectively, are adopted in this analysis.

Orientational Order Parameter of the α-Helical Backbone in Solution. Typical examples of the D NMR spectra of PBLG observed in the lyotropic liquid-crystalline state are illustrated in Figure 2. The N–D bond tightly fixed along the α-helix of PBLG through the intramolecular hydrogen bond, C*=O···D—N, gives rise to a doublet of peaks with a large separation ($\Delta\nu_N \simeq 250$ kHz) at room temperature (Figure 2a). In the biphasic equilibrium region, a sharp single peak appears in the center of the diagram in addition to the doublet due to the anisotropic phase, indicating that the molecular orientation is entirely lost in the isotropic state. Shown in Figure 2b is the D NMR spectrum of the C$^\alpha$–D bond: signals are sharper than those of the N–D bond, but the separation of the doublet ($\Delta\nu_\alpha$ = 15–18 kHz) is much smaller. The

Table I
Quadrupolar Splittings $\Delta\nu_\alpha$ and $\Delta\nu_N$ Observed for PBLG-N,α-d_2, Their Ratios $|\Delta\nu_\alpha/\Delta\nu_N|$, and the Order Parameter of α-Helical Axis S Calculated Therefrom

solvent	10^4M_v	v_x	temp, °C	$\Delta\nu_\alpha$, kHz	$\Delta\nu_N$, kHz	$10^2|\Delta\nu_\alpha/\Delta\nu_N|$	S
chloroform	6.8	0.30	21	18.92	259.5	7.31	0.971
			30	18.68	259.0	7.23	0.964
			45	18.63	256.2	7.29	0.957
			60	18.16	253.5	7.16	0.940
	5.7	0.25	30	18.21	250.8	7.26	0.936
		0.20	30	17.68	243.8	7.25	0.910
		0.15[a]	30	15.38	214.0	7.19	0.795
dichloromethane	6.8	0.20	30	17.68	241.3	7.33	0.905
DMF	5.7	0.35	30	17.77	245.0	7.25	0.914
			60	17.06	235.1	7.26	0.878
		0.30	30	16.97	235.2	7.22	0.875
		0.25	30	16.02	220.1	7.28	0.823

[a] The concentration corresponds to the biphasic equilibrium regime.

Table II
Geometrical Parameters of the α-Helical Backbone Estimated from the Observed $\Delta\nu_\alpha$ and $\Delta\nu_N$ Data[a]

bond	length, Å	bond angle	angle, deg	torsional angle	angle, deg
C^α—C^*	1.530	$\angle NC^\alpha C^*$	110.3	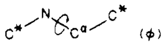	−62.5 (−68.1)
C^*—N	1.325	$\angle C^*NC^\alpha$	121.0		
N—C^α	1.453	$\angle C^\alpha C^*N$	115.0	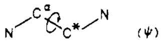	−42.3 (−38.1)
C^*=O	1.230	$\angle C^\alpha C^*O$	121.3 (120.5)		
C^α—C^β	1.530	$\angle NC^*O$	123.7 (124.5)	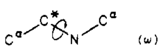	180.0
N—D	1.000	$\angle C^*ND$	123.2 (124.0)		
C^α—D^α	1.100	$\angle C^\alpha ND$	115.8 (115.0)		
		$\angle C^*C^\alpha C^\beta$	114.0 (111.0)		
		$\angle NC^\alpha C^\beta$	115.0 (111.0)		
		$\angle NC^\alpha D^\alpha$	108.9 (111.6)		

[a] Iterative calculations were carried out starting from Momany et al.'s parameter set.[16] Their values are indicated in parentheses where deviations are noted.

observed quadrupolar splittings can be related to the order parameter of the molecular axis by the expressions given in eq 1–3. In these expressions, the value of S varies rather sensitively with angles θ_N, ϕ_N, and θ_α. An accurate estimate of these angles is therefore very important. Since $\Delta\nu_N$ and $\Delta\nu_\alpha$ obtained from the same sample involve a common S value, the ratio of these splittings $|\Delta\nu_\alpha/\Delta\nu_N|$ should yield a geometrical relation comprising the above-mentioned angles. Samples of PBLG-N,α-d_2 with molecular weight of 6.8×10^4 and 5.7×10^4 were examined in chloroform, dichloromethane, and DMF. In DMF, the intermolecular association of PBLG is known to be least marked.[6] As shown in Table I, the ratio $|\Delta\nu_\alpha/\Delta\nu_N|$ remains nearly constant independent of solvent, concentration, and temperature. In general, location of the deuterium nucleus is difficult to assess. Use of the relation set forth above should lead to an improved estimate of the spatial orientation of the N–D and C^α–D bonds. As inspection of a molecular model reveals, the direction of the N–D bond varies quite sensitively with the bond angles around the carbonyl carbon. Similarly, bond angles around the α-methine carbon determine the orientation of the C^α–D bond. It may be reasonable to assume here that the deuterium nucleus is situated at an equal distance from the three heavy atoms bonded to C^α, i.e., C^β, C^*, and N. Bond lengths and bond angles other than those mentioned above were taken from Momany et al.'s paper.[15] The rotation angles around N–C^α (ϕ) and C^α–C^* (ψ) were adjusted to keep the molecular axis in an 18/5 helix with a screw pitch of 1.5 Å.[16] In the present treatment, the amide group was taken to be planar: thus, $\angle C^\alpha C^*O + \angle NC^*O = 2\pi - \angle C^\alpha C^*N$. We further assumed that $\angle C^\alpha C^*N$ (115.0°) was invariant. A set of angles thus optimized is listed in Table II, together with the bond lengths used in the calculation. Momany et al.'s values are indicated in parentheses. The deviations from Momany et al.'s set were found to be very trivial.[17] Values of the dihedral angles ϕ and ψ for the main chain were calculated to be −62.5° and −42.3°, being in close agreement with those (−63° and −42°) reported from the X-ray analysis by Blundell et al.[18] With the molecular geometry established in this manner, we obtain q_h = 178.3 kHz for the N–D bond and −12.93 kHz for the C^α–D bond. Values of the order parameter of the α-helical backbone estimated by using eq 1 are listed in the last column of Table I. In our preliminary analysis,[1a] we have used q_h = 192.9 kHz, a value larger by 8.2% than the present result. Accordingly, the order parameters are underestimated by this amount in the previous paper.

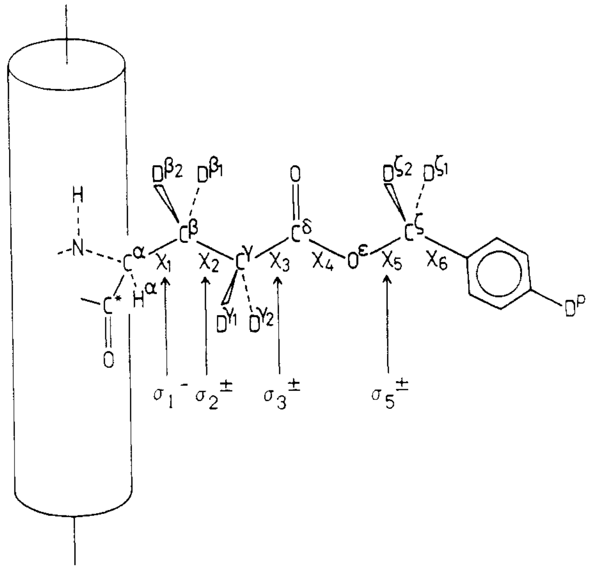

Figure 3. Schematic illustration of the side chain flanking the α-helical backbone of PBLG.

Side-Chain Conformation. A schematic illustration of the side chain flanking the α-helical backbone is given in Figure 3. Examples of the D NMR spectra obtained

Table III
Summary of Quadrupolar Splittings $\Delta\nu^{\text{obsd}}$ and the Order Parameter S for PBLG Having Selectively Deuterated Side Chains

solvent	v_x	temp, °C	$\Delta\nu^{\text{obsd}}$, kHz							S
			$\beta1$	$\beta2$	$\gamma1$	$\gamma2$	$\zeta1$	$\zeta2$	p	
1,4-dioxane	0.20	30	23.38	11.18	25.37	9.55	19.95	18.13	29.96	0.915
		55	24.00	11.20	23.90	10.75	17.49	19.31	25.94	0.897
		80	24.65	11.40	22.75	10.94	13.59	20.26	21.30	0.873
chloroform	0.30	30			27.20	10.84	18.82	15.58	24.83	0.975
	0.25	30			25.88	10.45	17.85	14.94	24.90	0.940
	0.20	30	23.88	12.02	25.24	10.11	17.30	14.40	24.07	0.908
		55	24.06	12.24	24.44	10.78	14.82	11.72	23.09	0.891
		80	24.06	12.24	23.83	11.13	12.93	9.01	22.33	0.871
	0.15	30					16.85	14.14	23.56	0.888
	0.15	30			22.75	9.10				0.820
m-cresol	0.20	30	29.79	1.20	11.76	20.75	21.70	10.20	25.75	0.900
		55	27.52	3.28	13.75	17.75	19.80	8.75	22.25	0.890
		80	25.98	5.86	15.50	15.75	19.00	7.18	18.50	0.870

Table IV
Bond Lengths, Bond Angles, and Rotational Angles Adopted for the Analysis of the Pendant Side Chain of PBLG

bond	length, Å	bond angle	angle, deg	bond	rot angle, deg	
					trans	gauche
C–C	1.530	$\angle C^\alpha C^\beta C^\gamma$	112.0[a]	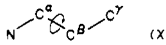 (χ_1)	180.4[e]	−75.0[e]
C–D	1.100	$\angle C^\beta C^\gamma C^\delta$	115.0[b]			
C^δ–O^ϵ	1.370	$\angle C^\gamma C^\delta O^\epsilon$	111.4[a]	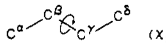 (χ_2)	180.0	±67.5[a]
O^ϵ–C^ζ	1.440	$\angle C^\delta O^\epsilon C^\zeta$	118.3[c]			
C^ζ–C^{ph}	1.450	$\angle O^\epsilon C^\zeta C^{ph}$	108.0[c]	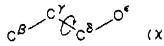 (χ_3)	180.0	±57.3[a]
		$\angle C^\alpha C^\beta D^\beta$	109.2[d]			
		$\angle C^\beta C^\gamma D^\gamma$	108.4[d]	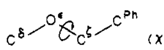 (χ_5)	180.0	±76.0[c]
		$\angle O^\epsilon C^\zeta D^\zeta$	110.2[d]			

[a] Reference 21a. [b] Reference 22. [c] Reference 21b. [d] Calculated by assuming a value of ∠DCD = 107.9°.[23] [e] Estimated from the D NMR splittings of the β-methylene group observed in 1,4-dioxane and chloroform. Somewhat larger displacement of rotational angles were obtained in *m*-cresol: 190.0° (trans) and −62.0° (gauche).

for PBLG-α,β-d_3, PBLG-γ-d_2, and PBLG-d_7 are shown in Figure 4. Under the given condition (20% v/v in chloroform, at 30 °C), all samples were found to be in the liquid-crystalline state. The quadrupolar splittings of the β- and γ-methylene deuterons can be identified as illustrated in the diagrams (Figure 4a and 4b). For PBLG-d_7, we adopted the assignment reported by Samulski et al.[2,3] (Figure 4c). It should be noted here that the two deuterons located on the same methylene carbons are stereochemically unequivalent and yield doublets with different splittings. Such conformational asymmetry becomes less marked for the ζ-deuterons.

Values of the quadrupolar splittings observed in 1,4-dioxane, chloroform, and *m*-cresol are summarized in Table III. The dielectric constant of the solvents increases in this order: 2.2, 4.9, and 11.8. The last two solvents are capable of forming hydrogen bonds with the carbonyl group of the side chain. The orientational order parameters of the helical axis estimated for given concentration and temperature are listed in the last column. As shown in eq 4 and 5, the ratio $\Delta\nu^{\text{obsd}}/S$ involves only contributions from the side-chain conformation. In Figure 5, these ratios are plotted against concentration v_x. The experimental values were found to remain nearly invariant with concentration for all C–D bonds. These observations are indicative of the fact that the average orientations, $\langle\cos^2\theta\rangle$, of the C–D bonds are unaffected by intermolecular interactions over the concentration range studied.[19]

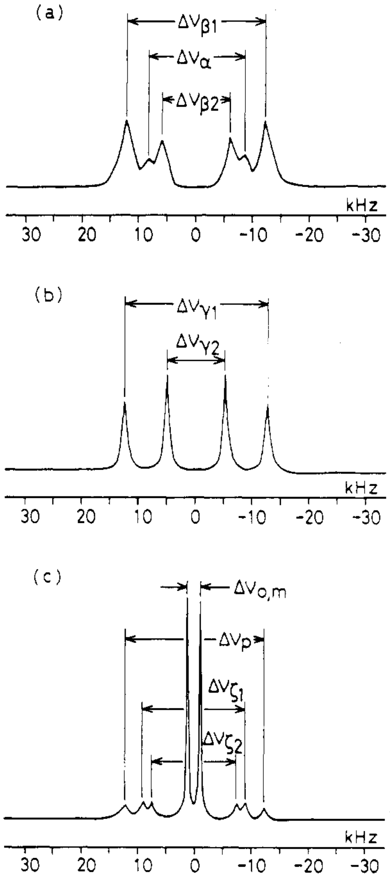

Figure 4. Examples of the D NMR spectra observed in chloroform at 30 °C: (a) PBLG-α,β-d_3, (b) PBLG-γ-d_2, and (c) PBLG-*benzyl*-d_7.

Geometrical parameters required for the description of the side-chain conformation (cf. Figure 3) are listed in Table IV. Conventional values were adopted for the bond lengths and bond angles of the skeletal chain and the ester group.[20,21] The ester C^δ–O^ϵ bond was taken to be trans. The angles for the articulated C–D bonds were calculated by assuming a value of ∠DCD = 107.9°, which was reported from the electron diffraction studies on *n*-propane.[22] For the C^α–C^β bond, the g^+ state is disallowed due to the severe steric conflict taking place between the γ-CH_2 group and the backbone. The rotation angles for χ_1 = t and g^- were

Table V
Values of the Statistical Weight Parameters Estimated for the Side Chain Flanking the α-Helical Backbone of PBLG in 1,4-Dioxane, Chloroform, and *m*-Cresol (v_x = 0.20)

statistical weight parameter	1,4-dioxane			chloroform			*m*-cresol		
	30 °C	55 °C	80 °C	30 °C	55 °C	80 °C	30 °C	55 °C	80 °C
σ_1^-	0.429	0.463	0.502	0.435	0.477	0.516	1.357	1.385	1.447
σ_2^+	0.000	0.049	0.093	0.000	0.062	0.135	0.746	0.761	0.664
σ_2^-	0.000	0.009	0.075	0.000	0.000	0.003	0.180	0.254	0.191
σ_3^+	0.598	0.850	1.200	0.610	0.770	0.880	0.590	0.545	0.480
σ_3^-	0.000	0.040	0.100	0.620	1.120	1.680	0.020	0.380	0.650
σ_5^+	0.210	0.260	0.300	0.370	0.420	0.460	0.245	0.320	0.660
σ_5^-	0.210	0.260	0.300	0.370	0.420	0.460	0.070	0.360	0.660

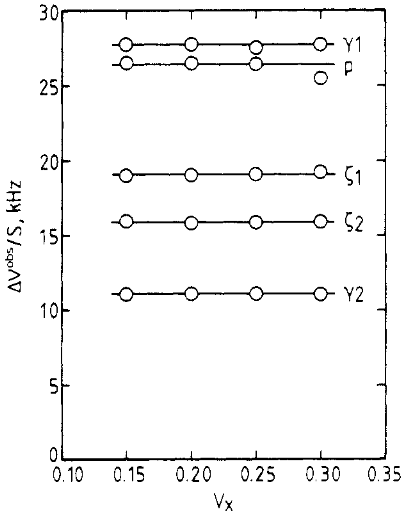

Figure 5. Variation of the ratio, $\Delta\nu^{\mathrm{obsd}}/S$, as a function of concentration, v_x, observed in chloroform at 30 °C. The corresponding C–D bond may be identified from the diagram shown in Figure 3.

determined from the observed D NMR splittings of the β-methylene group. Statistical weight parameters σ_i^+ and σ_i^- were assigned, respectively, to the g$^+$ and g$^-$ states of rotatable bond *i*, the weight of unity being given to the corresponding trans states (cf. Figure 3). As mentioned earlier, the side chains are conformationally asymmetric in the PBLG system, and thus in general, $\sigma_i^+ \neq \sigma_i^-$. Spatial arrangements such as $\chi_1\chi_2$ = tg$^-$ and g$^-$g$^+$ and $\chi_2\chi_3$ = g$^\pm$g$^\mp$ involve steric interactions between groups separated by more than four bonds. As inspection of a model reveals, these second-order interactions are highly repulsive. In this treatment, these high-energy conformations were ignored.

With geometrical parameters thus defined, the orientation of the individual C–D bonds, as expressed in terms of $\cos^2\theta$, may be calculated easily for all allowed spatial configurations. The relative importance of a given configuration can be customarily expressed by the product of statistical weight factors assigned to the constituent bonds. A sum of these products corresponds to the conformational partition function of the side chain:

$$Z = \sum_k (\prod_i s_i)_k \qquad (6)$$

where s_i represents the weight for bond *i*, i.e., 1 or σ_i, in the *k*th configuration (cf. Figure 3). In the actual procedure, statistical weight factors $\sigma_i^\pm$ were treated as variables within 0–1, the upper limit being set somewhat arbitrarily (e.g., the σ value of the *n*-alkane chain in the free state is ca. 0.5).[23] The average $\langle\cos^2\theta\rangle$ required in eq 4 and 5 may be obtained by

$$\langle\cos^2\theta\rangle = z^{-1}\sum_k[\cos^2\theta\,(\prod_i s_i)]_k \qquad (7)$$

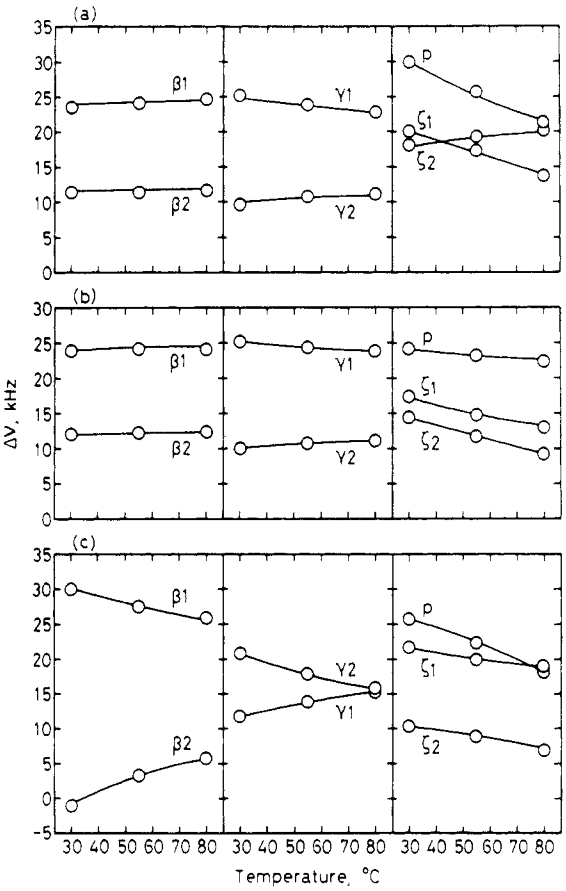

Figure 6. Temperature dependence of quadrupolar splittings Δν. The values observed at v_x = 0.20 in (a) 1,4-dioxane, (b) chloroform, and (c) *m*-cresol are shown by the open circles in the corresponding diagrams. The experimental results are well reproduced by the RIS simulation, as indicated by the solid curves.

In principle, the treatment may yield more than two sets of solutions. In the present example, however, we observed a unique convergence of the simulation. Substitution of the average $\langle\cos^2\theta\rangle$ in eq 4 may yield Δν with either a positive or negative sign. Comparison with the observed splittings requires only absolute values of Δν. Computations were iteratively repeated until the calculated values of $|\Delta\nu|$ reproduced those observed.

The results of the rotational isomeric-state (RIS) analysis are shown in Figure 6, where the observed temperature dependence of Δν values (open circles) is compared with that calculated (solid curves). Experimental data were derived from solutions of v_x = 0.20 in 1,4-dioxane (Figure 6a), chloroform (Figure 6b), and *m*-cresol (Figure 6c) over the temperature range 30–80 °C. In each diagram, the observed trends are satisfactorily reproduced by the RIS simulation described above. As shown by comparison, the solvent effect tends to be more marked toward the terminal of the side chain. The best-fit values of σ_i values

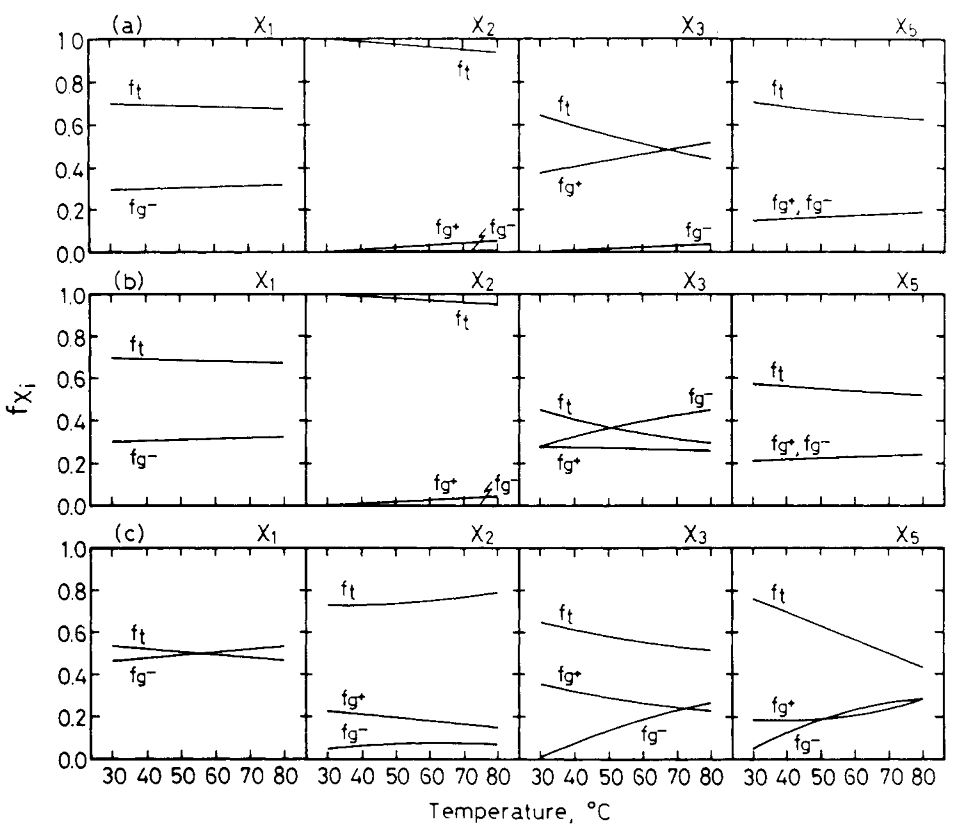

Figure 7. Bond conformation probabilities of the individual rotatable bonds estimated at $\upsilon_x = 0.20$ over a temperature range 30–80 °C: (a) 1,4-dioxane, (b) chloroform, and (c) *m*-cresol.

obtained by this analysis are summarized in Table V. A set of σ_i values thus derived immediately establishes a class of configurations permitted under given experimental conditions. The results obtained at 30 °C are shown in Table VI. Bond conformation probabilities estimated on this basis for the individual rotatable bonds are plotted in Figure 7 as a function of temperature.

In the first two solvents of Table VI, i.e., 1,4-dioxane and chloroform, the all-trans conformation was found to be the most preferred. These observations are not in accord with what was predicted from the conventional energy calculations.[24] As an inspection of a molecular model should reveal, the side chain prefers to take conformations extending toward the transverse direction with respect to the α-helical backbone. These characteristics are manifestly shown in the alteration of the bond conformation probabilities along the chain (Figure 7). While χ_1 and χ_3 are allowed to take gauche conformations to some extent, χ_2 is strictly confined to trans (see columns 3 and 4 of Figure 7). In parts a and b of Figure 7, the difference between these two solvents may be noted in the g^- conformation around C^γ–C^δ (χ_3). The disparity observed in the variation of $\Delta\nu_p$ and $\Delta\nu_\zeta$ values with temperature can be accounted for by the contribution from conformations such as ttg$^-$tt and ttg$^-$tg$^\pm$ in chloroform.

In *m*-cresol, preferences among conformations are very much different from those in the other solvents. Major differences may be noted in that (1) g$^-$tttt becomes more popular than the all-trans form and (2) an $\chi_2 = g^+$ conformation such as tg$^+$ttt exists in an appreciable amount. In general, *m*-cresol is known to exhibit a very specific solvent effect on PBLG.[10,25] The present analysis indicates that conformations around the inner bonds such as C^α–C^β (χ_1) and C^β–C^γ (χ_2) are also affected.

Conformational Space Exclusion by Surrounding Side Chains. As suggested by the experimental results described above, steric overlaps between the neighboring side chains may be substantial in the PBLG system. In Figure 8, the arrangement of side chains around the α-helical backbone is schematically illustrated by a radial projection. A given side chain (shaded circle) is surrounded by six immediate neighbors numbered from 1 to 6. Ten-

Table VI
Distribution of Conformers of the Side Chain Flanking the α-Helical Backbone of PBLG Estimated from Statistical Weight Parameters Given in Table V (30 °C)

conformation					fraction, %		
χ_1	χ_2	χ_3	χ_4	χ_5	1,4-dioxane	chloroform	*m*-cresol
t	t	t	t	t	30.9	18.0	14.5
t	t	t	t	g^+	6.5	6.6	3.6
t	t	t	t	g^-	6.5	6.6	1.0
t	t	g^+	t	t	18.4	11.0	8.6
t	t	g^+	t	g^+	3.9	4.1	2.1
t	t	g^+	t	g^-	3.9	4.1	0.6
t	t	g^-	t	t	0.0	11.1	0.3
t	t	g^-	t	g^+	0.0	4.1	0.1
t	t	g^-	t	g^-	0.0	4.1	0.0
t	g^+	t	t	t	0.0	0.0	10.8
t	g^+	t	t	g^+	0.0	0.0	2.7
t	g^+	t	t	g^-	0.0	0.0	0.8
t	g^+	g^+	t	t	0.0	0.0	6.4
t	g^+	g^+	t	g^+	0.0	0.0	1.6
t	g^+	g^+	t	g^-	0.0	0.0	0.4
g^-	t	t	t	t	13.2	7.8	19.7
g^-	t	t	t	g^+	2.8	2.9	4.8
g^-	t	t	t	g^-	2.8	2.8	1.4
g^-	t	g^+	t	t	7.9	4.7	11.6
g^-	t	g^+	t	g^+	1.6	1.8	2.9
g^-	t	g^+	t	g^-	1.6	1.8	0.8
g^-	t	g^-	t	t	0.0	4.8	0.4
g^-	t	g^-	t	g^+	0.0	1.8	0.1
g^-	t	g^-	t	g^-	0.0	1.8	0.0
g^-	g^-	t	t	t	0.0	0.0	3.6
g^-	g^-	t	t	g^+	0.0	0.0	0.9
g^-	g^-	t	t	g^-	0.0	0.0	0.2
g^-	g^-	g^-	t	t	0.0	0.0	0.1
g^-	g^-	g^-	t	g^+	0.0	0.0	0.0

Table VII
Conformational Energies Calculated for Some Preferred Arrangements Assuming Various Models for the Surrounding Side Chains and Comparison with Experimental Results

conformation					ΔE, kcal mol^{-1}			
χ_1	χ_2	χ_3	χ_4	χ_5	model 1	model 2	model 3	experimental[a]
t	t	t	t	t	0.23	0.00	*b*	0.00
t	t	t	t	g^+	1.56	1.33	*b*	0.94
t	t	t	t	g^-	1.55	1.50	*b*	0.94
t	t	g^+	t	t	1.58	1.31	1.56	0.31
g^-	t	t	t	t	0.00	*b*	0.00	0.51
g^-	t	g^+	t	t	0.98	0.78	*b*	0.82

[a] Estimated from the data in 1,4-dioxane ($\upsilon_x = 0.20$) at 30 °C. [b] Very large.

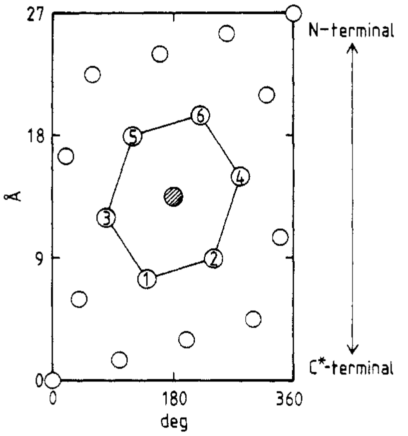

Figure 8. Lateral view of the α-helical PBLG as illustrated by the radial projection. A given side chain (shaded circle) is surrounded by the six nearest neighbors, numbered from 1 to 6.

tative calculations by assuming the surrounding side chains to be all methyl, i.e., R_{1-6} = Me, indicated that conformation $\chi_1\chi_2\chi_3\chi_4\chi_5 = g^-tttt$ was more stable than ttttt. Similarly, Piela et al.[26] have calculated the conformation of a glutamic acid side chain placed in the middle of a right-handed poly(L-alanine) α-helix (R_0 = Glu, R_{1-6} = Me) and stated that the $\chi_1\chi_2\chi_3 = g^-tt$ form should be the most stable. These results are apparently inconsistent with our experimental observations on PBLG, which suggest that ttttt is the most preferred form in nonpolar media such as 1,4-dioxane and chloroform. An attempt was made to elucidate the effect of interdependence between side-chain conformations in determining the preference among conformers (cf. Table VI). As may be easily shown by an inspection of a molecular model, steric conflicts, are severe, especially between side chains aligned in the direction connecting R_1–R_0–R_6 in Figure 8; e.g., when R_1 takes g^-tttt, R_0 cannot be placed in ttttt, and similarly R_0 interferes with R_6. The exact treatment of such a long-range interaction is very difficult in the present RIS scheme. To make calculations tractable, three simplified models were assumed for the surrounding side chains: (1) the nearest BLG side chains take the same conformations as those of the central one, (2) the conformation of the nearest neighbors is fixed in the most preferred all-trans form (cf. Table VI),[27] and (3) side chains R_1 and R_6 take g^-tttt, while the remaining groups (R_{2-5}) are kept in the all-trans form. Model 1 represents the scheme in which side-chain motions are highly cooperative, while models 2 and 3 correspond to the case in which side chains fluctuate in a less correlated manner with each other. The energy calculations were carried out for conformations comprising major fractions in 1,4-dioxane (Table VI): semiempirical energy expressions were taken from our previous work.[28] For long-range interactions between groups separated by more than five bonds, only the repulsive part of the energy functions was used; i.e., the cutoff distances were set at the sum of the van der Waals radii of the interacting atoms. Conformational energies estimated for the side chain R_0 are summarized in Table VII, where energies are expressed relative to the most stable conformation in each model.

The results obtained for model 1 were found to be nearly identical with those derived by setting R_{1-6} = Me (see above); e.g., g^-tttt is slightly more stable than ttttt. In model 2, g^-tttt is disallowed by the steric conflict with R_6, which is fixed in the all-trans form. Conformational energies are therefore expressed relative to the all-trans form. Except for the g^-tttt arrangement, the results obtained for model 2 closely parallel those of model 1, indicating that the inter-side-chain interactions are less severe in the direction other than R_1–R_0–R_6. In contrast to model 2, conformations such as ttttt, $ttttg^+$, $ttttg^-$, and g^-tg^+tt are eliminated in model 3 by the assignment of g^-tttt to R_1. As shown by comparison, ttg^+tt is least affected by the surrounding side chains. The experimental results listed in the last column of Table VII are intermediate between those of models 2 and 3. In fact, the observed fractions (cf. Table VI) can be reproduced by a proper distribution (e.g., model 2 × 0.308 + model 3 × 0.132) of contributions from these models. The results of calculations indicate that steric overlaps between adjacent side chains play an important role in determining the preference of conformations in the PBLG system. In fact, D NMR observations on copolymers of BLG-d_7 with γ-methyl L-glutamate (MLG) have revealed that the conformational restriction, as expressed by the number of conformations permitted, becomes less severe as the content of MLG residue increases.[29]

Conclusion

With side-chain conformations established as above, we can elucidate various characteristics of the PBLG molecules. The average separation of the phenyl group from the α-helical axis, as expressed by the center-to-center distance, should provide a simple measure for the extension of the side chain. The values were estimated to be 9.0 Å in 1,4-dioxane, 8.7 Å in chloroform, and 8.3 Å in *m*-cresol.

The lateral dimension of the α-helical PBLG rod may also be defined by the radius of gyration:

$$R_G = (\sum m_j r_j^2 / \sum m_j)^{1/2} \qquad (8)$$

where m_j represents the mass of group j, located at the distance r_j from the center of the α-helix. From the results shown in Table V, we obtain R_G = 6.6 Å in 1,4-dioxane, 6.4 Å in chloroform, and 6.5 Å in *m*-cresol. The average radius thus estimated tends to decrease gradually with temperature in all solvents: $d \ln R_G/dT \simeq -0.5 \times 10^{-3}$ K^{-1}. The values of R_G obtained above are substantially larger than those (3.5–4.8 Å) reported by Luzzati et al.[30] by using the SAXS technique. Ishimuro et al.[31] have introduced a correction term in consideration of the electron cloud of the surrounding solvent molecules in their treatment of SAXS data of PMLG. The aforementioned discrepancy between D NMR and SAXS values can be improved somewhat by adopting similar corrections. Teramoto et al.[32] have estimated the diameter of α-helical PBLG from the viscosity–molecular weight relation. The value of 15.6 Å thus derived is reasonably consistent with the present results.

The other conformation-dependent properties such as the average orientation of the terminal phenyl group, which is important in determining the surface chirality of the PBLG rod, or dielectric properties of the side chain can be easily elucidated. The results relating to these topics will be reported in a forthcoming paper.[33]

Acknowledgment. We appreciate the help received from Prof. T. Oshima of our institute during the preparation of our deuterated PBLG samples. We are also grateful to Dr. H. Saito of the National Cancer Center Research Institute for his help in the solid-state NMR measurements on PBLG-*N-d*. This work was supported in part by a Grant-in-Aid for scientific research on priority areas, new functionality materials design, preparation, and control by The Ministry of Education, Science and Culture (63604531).

Registry No. PBLG (SRU), 25038-53-3; PBLG (homopolymer), 25014-27-1; NCA, 3190-71-4.

References and Notes

(1) (a) Yamazaki, T.; Abe, A. *Polym. J.* **1987**, *19*, 777. (b) Yamazaki, T.; Horiuchi, S.; Watanabe, J.; Abe, A.; Ono, H. *Polym. Prepr. Jpn.* **1987**, *36*, 1766.
(2) Samulski, E. T. *J. Phys., Paris* **1979**, *40*, C3–471.
(3) Czarniecka, K.; Samulski, E. T. *Mol. Cryst. Liq. Cryst.* **1981**, *63*, 205.
(4) Sohma, J.; Tabata, M. *Mol. Cryst. Liq. Cryst.* **1981**, *68*, 89.
(5) (a) Abe, A.; Furuya, H.; Yoon, D. Y. *Mol. Cryst. Liq. Cryst.* **1988**, *159*, 151. (b) Abe, A; Furuya, H. *Polym. Bull.* **1988**, *19*, 403.
(6) Doty, P.; Bradbury, J. H.; Holtzer, A. H. *J. Am. Chem. Soc.* **1956**, *78*, 947.
(7) (a) Hilton, M. A.; Barnes, F. W.; Henry, S. S.; Enns, T. W. *J. Biol. Chem.* **1954**, *209*, 743. (b) **1956**, *219*, 833.
(8) Whelan, D. J.; Long, G. J. *Aust. J. Chem.* **1969**, *22*, 1779.
(9) Tsutsumi, A.; Perly, B.; Forchioni, A.; Chachty, C. *Macromolecules* **1978**, *11*, 977.
(10) Toriumi, H.; Yamazaki, T.; Abe, A.; Samulski, E. T. *Liq. Cryst.* **1986**, *1*, 87.
(11) Chapman, G. E.; Campbell, T. D.; McLaughlin, K. A. *Nature* **1970**, *225*, 639.
(12) Chiba, T. *Bull. Chem. Soc. Jpn.* **1965**, *38*, 259.
(13) Poliks, M. D.; Park, Y. W.; Samulski, E. T. *Mol. Cryst. Liq. Cryst.* **1987**, *153*, 321.
(14) Emsley, J. W. *Nuclear Magnetic Resonance of Liquid Crystals*; NATO ASI Series: Dordrecht, 1985.
(15) Momany, F. A.; McGire, R. F.; Burgess, A. W.; Scheraga, H. A. *J. Phys. Chem.* **1975**, *79*, 2361.
(16) Mirau, P. A.; Bovey, F. A. *J. Am. Chem. Soc.* **1986**, *108*, 5130.
(17) In the previous calculation[1b] with our $(e^2qQ/h)_{ND}$ value (190.0 kHz), we noted some significant deviation from Momany et al.'s set:[15] $\angle C^{\alpha}C^{*}O = 129.30°$ and $\angle NC^{*}O = 115.7°$. Such difficulties have been dissolved by adoption of Poliks et al.'s $(e^2qQ/h)_{ND}$ value.[13]
(18) Blundell, T.; Barlow, D.; Borkakoti, N; Thornton, J. *Nature* **1983**, *306*, 281.
(19) The average separation of helical rods may be calculated by assuming a regular hexagonal array. At $v_x = 0.20$, the distance is estimated to be 28.7 Å, being sufficiently larger than the maximum diameter (22.4 Å, cf. sequence) of a PBLG molecule with fully extended side chains.
(20) (a) Abe, A. *J. Am. Chem. Soc.* **1984**, *106*, 14. (b) Abe, A.; Miura, I.; Furuya, H. *J. Phys. Chem.* **1987**, *91*, 6496.
(21) Morrison, J. D.; Robertson, J. M. *J. Chem. Soc.* **1949**, *17*, 1001.
(22) Iijima, T. *Bull. Chem. Soc. Jpn.* **1972**, *45*, 1291.
(23) Abe, A.; Jernigan, R. L.; Flory, P. J. *J. Am. Chem. So.* **1966**, *88*, 631.
(24) Yan, J. F.; Vanderkooi, G.; Scheraga, H. A. *J. Chem. Soc.* **1968**, *49*, 2713.
(25) (a) Toriumi, H.; Kusumi, Y.; Uematsu, I.; Uematsu, Y. *Polym. J.* **1979**, *11*, 863. (b) Toriumi, H.; Minakuchi, S.; Uematsu, I.; Uematsu, Y. *J. Polym. Sci., Phys. Ed.* **1981**, *19*, 1167.
(26) Piela, L.; Nemethy, G.; Scheraga, H. A. *Biopolymers* **1987**, *26*, 1273.
(27) A similar model has been empolyed by Suter et al. in their treatment of poly-4-methylpentene-1, which carries bulky pendant groups such as $CH(CH_3)_2$. Wittwer, H.; Suter, U. W. *Macromolecules* **1985**, *18*, 403.
(28) Abe, A.; Yamazaki, T. *Biopolymers* **1988**, *27*, 985.
(29) Yamazaki, T.; Abe, A.; Ono, H.; Toriumi, H. *Biopolymers*, in press.
(30) Luzzati, V.; Cesari, M.; Spach, G.; Masson, F.; Vincent, J. H. *J. Mol. Biol.* **1961**, *3*, 560.
(31) Ishimuro, Y.; Yamaguchi, S.; Hamada, F.; Nakajima, A. *Biopolymers* **1981**, *20*, 2499.
(32) Teramoto, A.; Fujita, H. *Adv. Polym. Sci.* **1975**, *18*, 65.
(33) Abe, A.; Yamazaki, T., to be published.

Orientational Order of α-Helical Poly(γ-benzyl glutamate) in the Lyotropic Liquid-Crystalline State. Comparison of Theory with Experiments

Akihiro Abe* and Toshimasa Yamazaki

Department of Polymer Chemistry, Tokyo Institute of Technology, 2-12-1 Ookayama, Meguro-ku, Tokyo 152, Japan. *Received June 9, 1988; Revised Manuscript Received October 14, 1988*

ABSTRACT: The orientational order parameter S was determined for α-helical PBG in the lyotropic liquid-crystalline state by using the deuterium NMR technique. PBG-*N-d* samples having axial ratios of x = 185, 121, and 32 were compared. The measurements were extensively carried out in dimethylformamide, in which intermolecular association of the solute is known to be very weak. The value of S decreases gradually on dilution until the upper equilibrium concentration (B point) is reached where the locus of data points eventually discontinues. The concentration dependence of S was compared with those derived from theories proposed by Onsager, by Flory and Ronca, and by Khokhlov and Semenov. None of these theories can predict satisfactorily both the observed critical concentration and the order parameter at the transition. The orientational distribution functions derived from these theories are also reported.

Introduction

In the preceding paper in this issue[1] (hereafter referred to as paper 1), the deuterium NMR technique has been extensively employed in studying the oritentational ordering of PBLG molecules in the lyotropic liquid-crystalline state. The deuterium atoms incorporated in the